Supporting Information

Interfacial Passivation of Perovskite Solar Cells by Reactive Ion Scavenger

Hakimeh Teymourinia,[1,2,†] Cedric Gonzales,[1,†] Juan Jesús Gallardo,[3] Masoud Salavati-Niasari,*[2] Juan Bisquert,[1] Javier Navas,[3] Antonio Guerrero*[1]

1 Institute of Advanced Materials, Universitat Jaume I, 12006, Castello, Spain

2 Institute of Nano Science and Nano Technology, University of Kashan, Kashan, P. O. Box. 87317-51167, I. R. Iran

3 Departamento de Química Física, Facultad de Ciencias, Universidad de Cádiz, E-11510 Puerto Real (Cádiz), Spain

† Both authors contributed equally

Email: salavati@kashanu.ac.ir (M. Salavati-Niasari,), aguerrer@uji.es (A. Guerrero)

Index

Methods

1. Materials and precursor solutions

All materials were used as received: FTO glasses (2.5 × 2.5 cm^2 Pilkington TEC15, ~15 Ω/sq resistance), CH_3NH_3I (DYESOL), PbI_2 (TCI, 99.99%), TiO_2 paste (Dyesol 30NRD, 300 nm average particle size), and Spiro-OMeTAD (Merck). The $MAPbI_3$ precursor solution is prepared as reported previously. [11] A solution of DMF (1 mL, 50 wt %) is prepared containing MAI (235 mg), PbI_2 (681.5 mg) and DMSO (95 μL). The perovskite precursor solution (50 μL) was spin-coated in a one-step setup at 4000 rpm for 50 s. During this step, DMF is selectively washed with non-polar diethyl ether just before the white solid begins to crystallize in the substrate. Afterward the substrate was annealed at 100 °C for 3 min). The Spiro-OMeTAD solution for devices was prepared by dissolving 72.3 mg of Spiro-OMeTAD in 1 ml of chlorobenzene followed by adding stock solution of 17.5μL of 520 mg/ml of lithium bis-(trifluoromethylsulfonyl) imide and 28.8 μL of 4-tert-butylpyridine (TBP) in acetonitrile.

2. Photovoltaic device fabrication

All fabrication steps were following through inside the glovebox with constant oxygen and water content.[1] Photovoltaic devices fabrication starts with etching FTO with zinc powder and HCl (2M) followed by cleaning with Hellmanex solution and rinsed with Milli-Q water and ethanol. Afterward, the substrates were sonicated for 15 min in ethanol, acetone, and dried. Finally, the substrates were treated in a $UV-O_3$ chamber for 15 min. Spray pyrolysis was used to deposit TiO_2 compact layer onto the FTO, the temperature was fixed at 450 ℃. Titanium diisopropoxide bis(acetylacetonate) solution diluted in ethanol with oxygen as the carrier gas was used as a precursor. The diluted TiO_2 paste was spin-coated at 2000 rpm during 10 s on the compact layer to form a mesoporous TiO_2 layer. After drying at 100 ℃ for 10 min, the TiO_2 mesoporous layer was cooked at 500 ℃ for 30 min and cooled to room temperature. The perovskite precursor solution was spin-coated using chlorobenzene as antisolvent and bake at 100 ºC for 10 min. For hole selective layer was prepared by spin coating a solution of Spiro-OMeTAD at 3000 rpm for 10 s. Then, the top contact was evaporated on the top of the Spiro layer composed by either Au (85 nm) for reference device or silver (from 0.5 to 5 nm) followed by gold (85 nm) at a base pressure of $1 \cdot 10^{-6}$ and $1 \cdot 10^{-5}$ mbar.

3. Device characterization

Photovoltaic devices were first characterized using an Abett Solar simulator under 1 Sun illumination. A calibrated Si solar cell was used to fix light intensity at 100 mW cm^{-2}. Devices were measured using a mask to define an active area of 0.11 cm^2. Further electrical tests were carried out during a period of 30-60 minutes in a dry box filled with air with relative humidity < 0.1 % with devices encapsulated by using a Scotch tape (3M).

4. Performance parameters Statistics

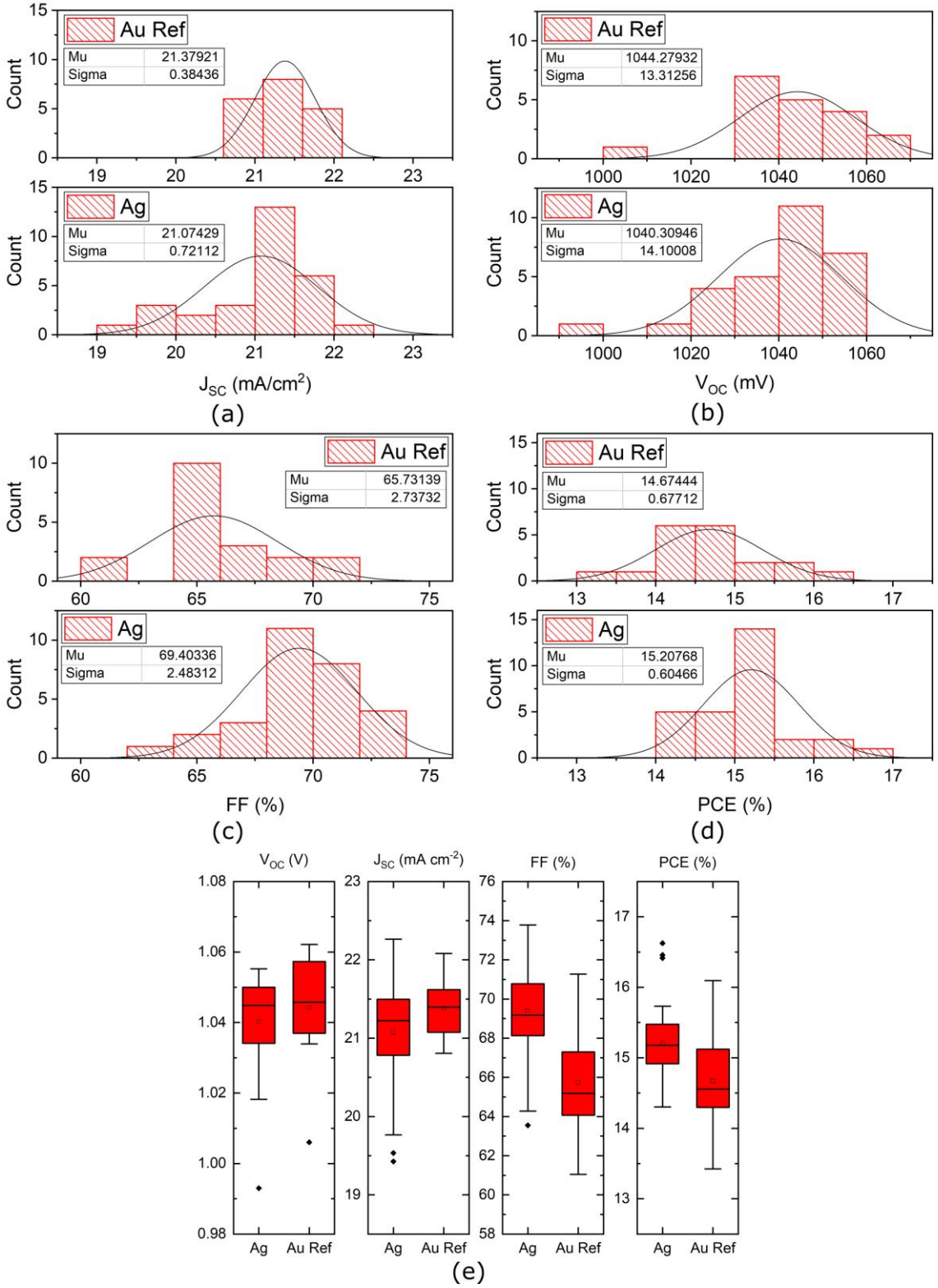

Figure S1: Performance parameters statistics of 20 devices fabricated with top contact containing Au and Ag (1 nm)/Au a) V_{oc}, b) J_{sc}, c) FF, d) PCE and e) Summary of all parameters.

5. Polarization protocol and IS measurement

To promote the chemical reactivity of the interface and its kinetics, the sequence of the measurements was completed following a protocol under two different environment conditions. Cyclic Voltammetry (CV) is measured in the dark with 9 different scan rates (0.01-10 V/s), starting from fast scan rate (10 V/s) to avoid irreversible modification in the device during long measuring times. 2 cycles are recorded 0 V (fresh) → 1V→ -1V→ 0V. The same sequence is repeated under illumination conditions and these results are shown in Figure 1b and 1e. The complete sequence dark and illumination is repeated once and results under illumination are shown in Figure 1c and 1f. The measurement typically takes 30 min from initial measurement to final.

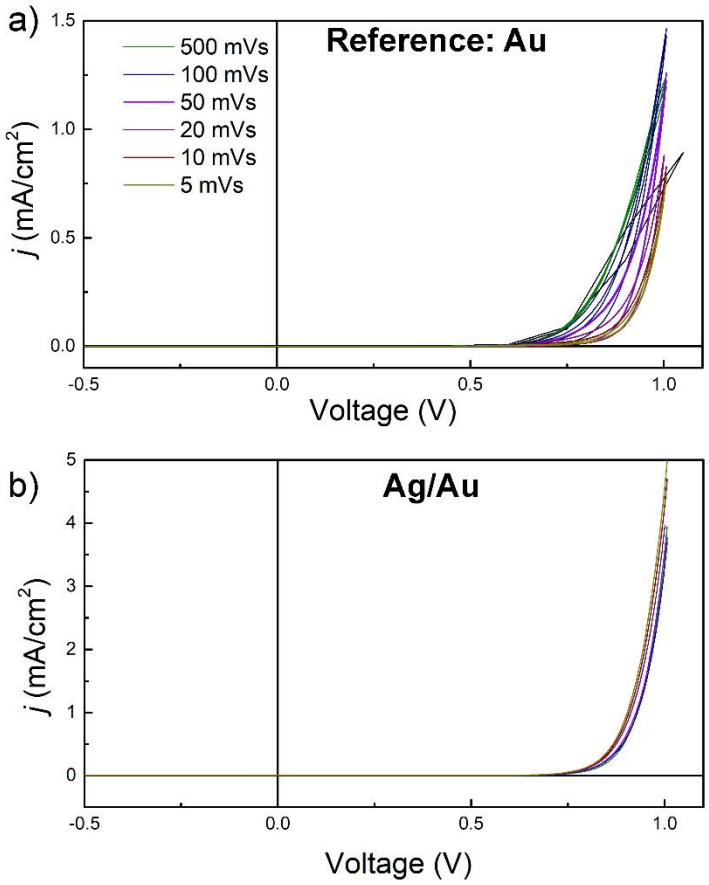

Figure S2. J-V curves of a reference device (a) and a devices containing a 2 nm of Ag buffer layer (b) after characterization using protocol described in the methods.

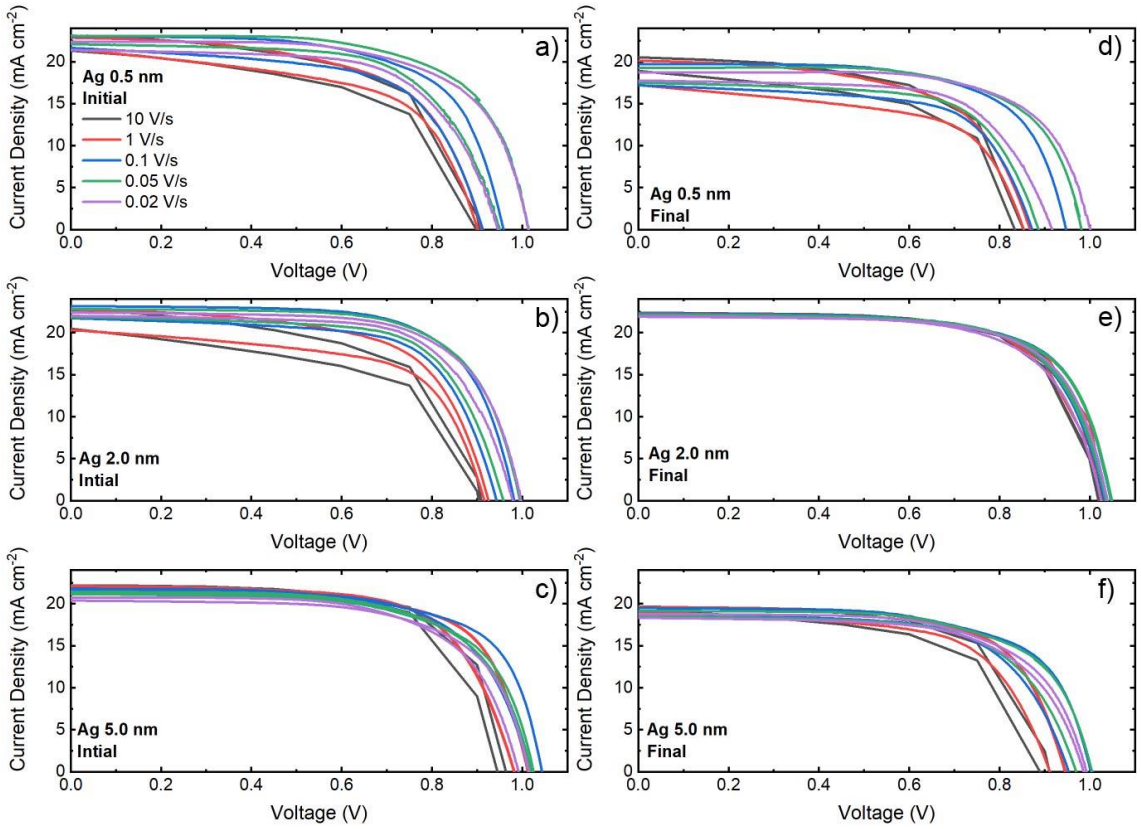

Figure S3: *J-V* curves of devices prepared with different thickness of Ag buffer layer. a), b) and c) corresponds to fresh samples and d), e) and f) the same samples after polarization under using positive voltages during J-V curves and light.

Impedance spectroscopy measurements were performed an Autolab PGSTAT-30 equipped with a frequency analyzer module. A DC voltage is applied and a small AC perturbation of 20 mV is overimposed. The differential current output is measured and the impedance and capacitance is analyzed using Z-View software. Measurements were carried out at in the dark using a fresh sample that has not been polarized before. The IS measuring sequence applies a DC voltage as follows 0 V (fresh) →200 mV→0V. This sequence is repeated once for Figure 3e and 3f.

6. Degradation Experiments

Whilst the selected perovskite formulation (MAPI) simplifies studies related to the understanding of physical and chemical processes it is not well suited for degradation experiments. Light induced degradation due to phase segregation and bleaching of the bulk of the perovskite is still observed. Further work using more stable perovskite formulations are in progress in our research group. We next move to understand the chemical effect of the Ag buffer layer between the Spiro-OMeTAD and Au.

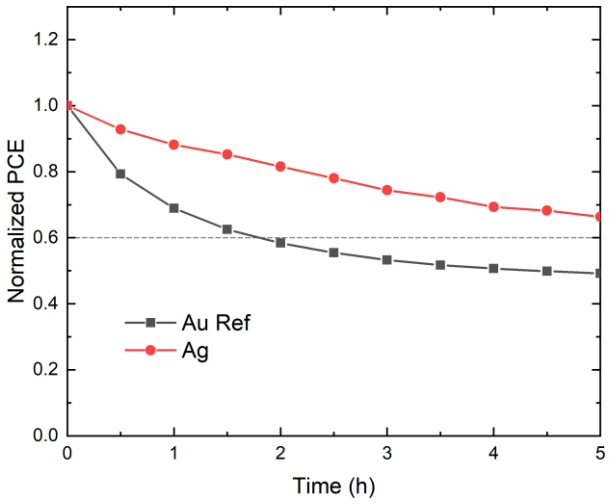

Figure S4: Representative initial performance decay of devices fabricated in this work under Maximum Power Point tracking conditions at 100 mWcm^{-2}.

7. XPS Measurements

X-ray photoelectron spectroscopy (XPS) was used to study the chemical bonding states of the Ag in the samples as described in the main text. The spectra were recorded using a Specs® Phoibos 150 MCD spectrometer, with monochromatic Al-Kα radiation (1486.6 eV) and a 20 eV pass energy. The binding scale was referred to the C 1s signal at 284.8 eV, and given with an accuracy of 0.1 eV. Here, we have developed a method to analyze interfacial reactivity in real devices by delamination of the top metal/Spiro interface, the result of such process is shown in Figure 2a. During preparation of the sample for XPS a device (fresh or stressed) is covered by a tape (3M) by pressing the sticking side of the tape towards the top electrodes. Then, the tape is carefully removed and delamination is promoted from the weakest interface available, Spiro-OMeTAD/top contact. The result of this delamination leaves a substrate with the perovskite and Spiro layer and the tape with the top contact (Au or Ag/Au). With this methodology for sample preparation the top surface of the metal corresponds to the material which was in close contact with the Spiro-OMeTAD in the device. The surface sensitive technique XPS is used to provide chemical information on the few top layers of the metal, hence, providing useful chemical reactivity information on the Spiro-OMeTAD/metal interface.

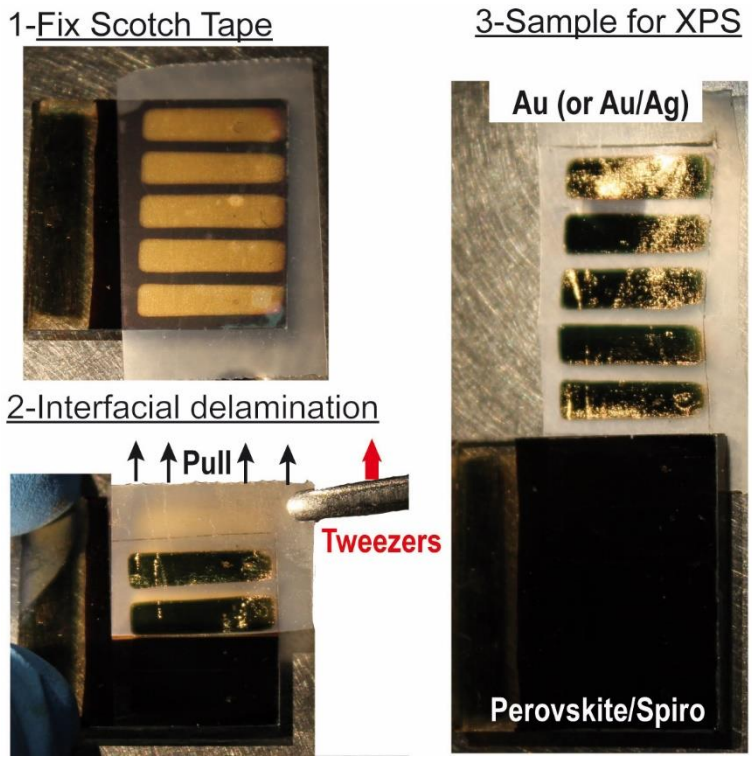

Figure S5: Steps followed to expose Spiro-OMeTAD/Top contact interface to prepare the sample for XPS analysis.

Figure 2b shows the Ag 3d high resolution XP spectrum of a Ag sample that has been stressed under bias and light and this is compared with a reference sample of Ag (100 nm) on FTO. The spectrum of the Ag reference sample shows two well-defined peaks. The binding energy (BE) values at the peak of the Ag $3d_{5/2}$ and $3d_{3/2}$ signals were about 367.9 and 373.9 eV, respectively, which means a separation for the spin-orbit components of about 6.0 eV. These values are typical for pure metallic Ag.[2] Moreover, a slight shift is observed in the signal obtained from polarized Ag device. Both spin-orbit components of the Ag 3d signal are shifted to a higher BE, which is evidence of the presence of oxidized Ag species. This oxidized species of Ag is generated as a result of Ag-halogen bonds.[3] The contribution of Ag $3d_{5/2}$ to the polarized Ag appears at a BE of about 368.2 eV, which matches with values previously reported for AgI.[4-8] Importantly, satellites are also observed at higher BE of each spin-orbit component for the Ag reference sample, the presence of these satellites is only typical for metallic Ag,[9] and the sample used as a reference was prepared without the presence of iodine or any oxidant agent. These satellites may be due to a collective excitation of the electrons in the embedding matrix, i.e. to the generation of a plasmon, when a core electron is removed.[9] The separation between the Ag $3d_{3/2}$ components and its satellite is about 3.85 eV, which is coherent with previous values reported for satellites in XP spectra for metal Ag due to plasmon losses.[10] Moreover, the presence of iodine in the Ag contact was analysed in order to observe the formation of Ag-I bonds and prove the diffusion of ions across the Spiro-OMeTAD layer.

Figure 2c shows the I 3d signal obtained. The BE at the maximum of the I $3d_{5/2}$ and $3d_{3/2}$ signals was found to be about 618.5 and 630.0 eV, respectively, which means a separation for the spin-orbit components of about 11.5 eV. These values are typical for the presence of I^- species [2, 8]. Thus, the evidence of I^- and the presence of Ag^+ in the contacts are evidence of the formation of Ag-I bonds. In turn, the Pb signal was analysed to rule out the presence in the tape of MAPI due to the delamination process. Typically, the 4f region, at about the 145-135 eV range, is analysed to determine the presence of Pb. Two spin-orbit components are usually observed with a separation of about 5 eV. As Figure 2d shows, no signal was observed in this range, so the presence of Pb in the Ag contact is negligible.

Due to the handling time between device fabrication and sample measurement by XPS in the order of 7 days AgI formation occur. A comparison by XPS of a non-polarized sample and a sample polarized using the measurement protocol is shown in Figure SI6. The Ag 3d high resolution XP spectrum (a) of a Ag sample that has been stressed under bias and light and this is compared with the non-polarized sample of Ag in a solar cell. For both samples, the binding energy (BE) values at the peak of the Ag $3d_{5/2}$ and $3d_{3/2}$ signals were about 367.9 and 373.9 eV, respectively, which means a separation for the spin-orbit components of about 6.0 eV. As is observed, the chemical state bonding of Ag in both samples is similar. Also, we can observe the signal of I 3d for both samples in Figure SI5(b). Again, no significant differences are found for the samples, so the chemical bonding state for I is similar in both samples. Finally, Figure S5(c) shows the signal for Pb 4f. No signal was observed in this zone, so the presence of Pb in the Ag contact is negligible in both samples. Therefore, we can conclude that AgI layer also form when devices are kept in the dark during several days.

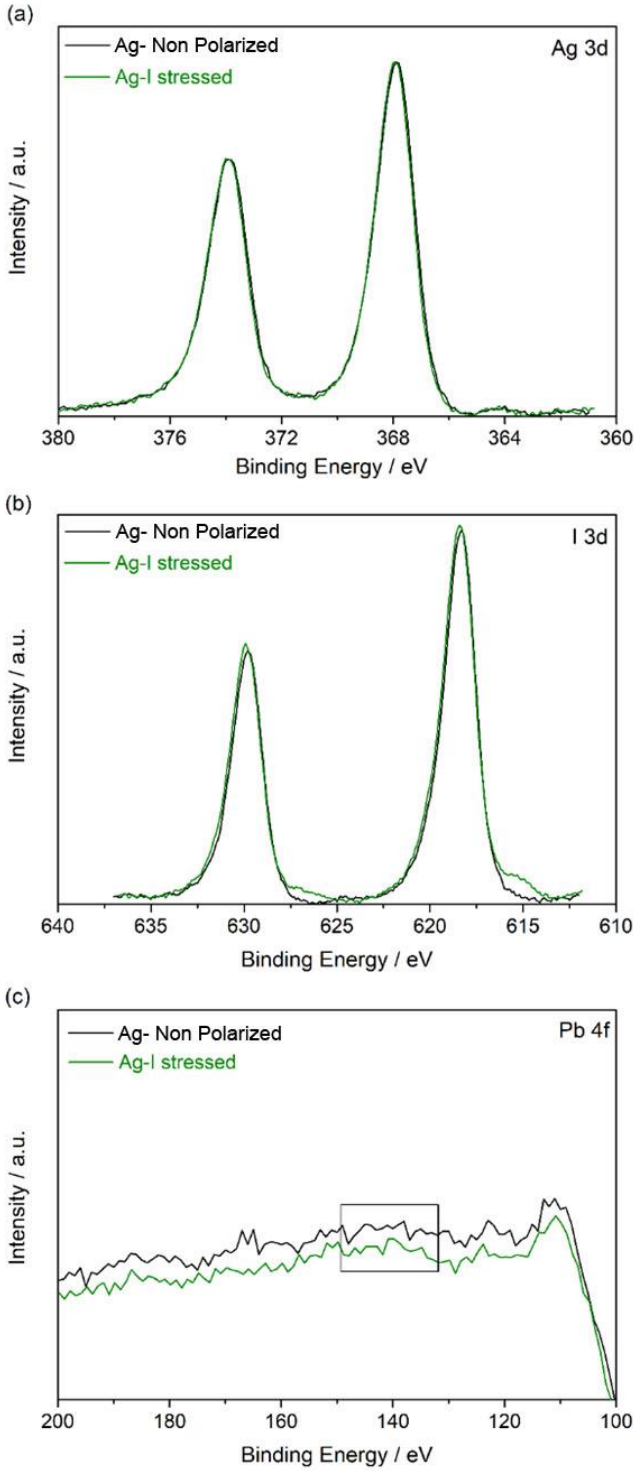

Figure S6: XPS signals comparison of the delaminated top contact in a non-polarized and stressed photovoltaic device containing a buffer layer of Ag (2 nm).

8. References

1. Tiihonen, A.; Miettunen, K.; Halme, J.; Lepikko, S.; Poskela, A.; Lund, P. D.,

Critical analysis on the Quality of Stability Studies of Perovskite and Dye Solar Cells. *Energy Environ. Sci.* **2018**, *11*, 730-738.

2. Naumkin, A. V.; Kraut-Vass, A.; Gaarenstroom, S. W.; Powell, C. J., *in NIST Standard Reference Database 20, Version 4.1, Gaithersburg* **2012**.

3. Zheng, Z.; Liu, A. R.; Wang, S. M.; Huang, B. J.; Ma, X. M.; Zhao, H.; Li, D. P.; Zhang, L. Z., In Situ Fabrication of AgI Films on Various Substrates. *Mater. Res. Bull.* **2008**, *43*, 2491-2496.

4. Jonjana, S.; Phuruangrat, A.; Thongtem, S.; Thongtem, T., Synthesis of AgI/Bi2MoO6 Heterojunctions and Their Photoactivity Enhancement Driven by Visible Light. *Mater. Lett.* **2016**, *175*, 75-78.

5. Li, X. X.; Fang, S. M.; Ge, L.; Han, C. C.; Qiu, P.; Liu, W. L., Synthesis of Flower-Like Ag/AgCl-Bi2MoO6 Plasmonic Photocatalysts with Enhanced Visible-Light Photocatalytic Performance. *Appl. Catal., B* **2015**, *176*, 62-69.

6. Ye, H. F.; Lin, H. L.; Cao, J.; Chen, S. F.; Chen, Y., Enhanced Visible Light Photocatalytic Activity and Mechanism of BiPO4 Nanorods Modified with AgI Nanoparticles. *J. Mol. Catal. A: Chem.* **2015**, *397*, 85-92.

7. Chen, Q. F.; Shi, W. M.; Xu, Y.; Wu, D.; Sun, Y. H., Visible-Light-Responsive Ag-Si Codoped Anatase TiO2 Photocatalyst with Enhanced Thermal Stability. *Mater. Chem. Phys.* **2011**, *125*, 825-832.

8. Moulder, J. F.; Stickle, W. F.; Sobol, P. E.; Bomben, K. D., *Handbook of X-ray Photoelectron Spectroscopy*. Perkin-Elmer Corporation, Physical Electronics Division: Eden Prairie, Minnesota, USA, 1992.

9. Eckardt, H.; Fritsche, L., Theoretical Explanation of the Xps Satellite Structure of Elementary Metals - Application to Ag. *Solid State Commun.* **1985**, *54*, 405-407.

10. Das, S.; Gersten, J. I.; Weisz, Z.; Resto, O.; Many, A.; Goldstein, Y., Interference Effect in Electron-Energy-Loss Spectroscopy. *Phys. Rev. B* **1989**, *39*, 11251-11258.